


Tensor current renormalization in the RI' scheme at four loops

J. A. Gracey 

*Theoretical Physics Division, Department of Mathematical Sciences, University of Liverpool,
P.O. Box 147, Liverpool, L69 3BX, United Kingdom*

 (Received 9 September 2022; accepted 26 September 2022; published 19 October 2022)

To assist the matching of lattice field theory results to the high energy continuum limit we evaluate the Green's function where the tensor quark bilinear operator is inserted at zero momentum in a quark 2-point function for an arbitrary covariant gauge. This is carried out in both the $\overline{\text{MS}}$ and RI' schemes to four loops. The tensor current anomalous dimension is also calculated to four loops in both schemes for an arbitrary color group.

DOI: [10.1103/PhysRevD.106.085008](https://doi.org/10.1103/PhysRevD.106.085008)

I. INTRODUCTION

The Standard Model (SM) is generally accepted to be the core theory that describes particle dynamics operating at the current energy scales of the Large Hadron Collider (LHC). However, as data gathering increases over the next few years it is expected that discrepancies between experimental results and SM predictions will emerge. This is on top of the known difficulty in reconciling small neutrino mass observations with the present neutrino content of the SM. Another aspect of the Standard Model that is the subject of intense study centers on determining the precise numerical elements of the Cabibbo-Kobayashi-Maskawa (CKM) matrix which governs quark mixing and underlies CP violation. Ensuring that the independent parameters are calculated accurately theoretically based on the Standard Model is an important foundation to finding a discrepancy with experimental measurements. Equally if differences are discovered one question that arises is what extension to the SM will explain the new observations. In this respect one major activity centers on constructing effective field theories that use the present SM particle content to build dimension five and six operators. These operators can have CP violating or other properties, for instance. One subset of such effective theories is to incorporate extra interactions with Lorentz structures different from those already in the Standard Model. For example, the SM has vector-axial vector interactions. However at an early stage of the SM development an alternative structure was considered that involved a tensor current. This was eventually excluded by experiment. In seeking to explore beyond the SM at current

LHC energies, however, tensor couplings have become an area of interest again. For example tensor couplings have been used to examine β decay of the nucleon in addition to beyond the SM CP violation searches. Its effect is manifest in the neutron electric dipole moment. Similar tensor couplings are also of interest in rare B decays as well as being included in SM effective theories in order to provide the freedom to cover the parameter search space as widely as possible ahead of more precise experimental data. Further background to theoretical aspects of these issues can be found, for example, in [1–3]. Indeed the use of tensor couplings in effective field theory extensions of the SM have been discussed recently in [4].

One of the main theoretical tools used to determine precise values of the various matrix elements that are central to these SM studies is lattice gauge theory where the related Green's functions are calculated numerically to very high accuracy. However, as the underlying field theory of the strong sector, quantum chromodynamics (QCD), is regularized by discretizing continuous spacetime lattice results have to be extrapolated to the continuum limit by reducing the lattice spacing. Taking such a limit is not straightforward but to assist with error analyses any numerical evaluation of a Green's function has to be consistent with its known high energy behavior. In other words lattice results have to match onto the same Green's function but computed by contrast directly in the continuum perturbative theory. The latter can be deduced using standard methods to evaluate Feynman integrals but to ensure precision matching and error analysis, having the matrix elements to as high a loop order as possible is important. There has been a large industry producing such perturbative calculations over the last few decades particularly in the case of operator insertions in 2-point functions. For instance, see [5–11] for the early developments. In essence there are two classes of such Green's functions. One is where an operator is inserted at zero momentum [5–7].

Published by the American Physical Society under the terms of the Creative Commons Attribution 4.0 International license. Further distribution of this work must maintain attribution to the author(s) and the published article's title, journal citation, and DOI. Funded by SCOAP³.

The other configuration is where the insertion is at nonzero momentum and additionally the momenta of the other external fields are nonzero [8–11]. While the latter class corresponds to a nonexceptional momentum configuration it is technically more difficult to compute high loop order corrections in this instance. By contrast Green's functions with operators at zero momentum insertion in a 2-point function effectively equate to a 2-point rather than a 3-point calculation and, moreover, can be determined to much higher orders perturbatively.

This is the main aim of this article where given the importance of the tensor current in QCD for exploring beyond the Standard Model we will compute the Green's function with that operator inserted at zero momentum at four loops. This will extend the equivalent three loop exercise of 20 years ago [7], which has been used in various lattice analyses that are focused on understanding the various SM extensions mentioned earlier such as B meson decays, β decay of nucleons, electric dipole moments of nucleons and the J/ψ decay constant. See, for example, [12–18] for several instances including the recent results of [19,20]. Equally there are also applications of the tensor current to effective field theory formulations of the SM [21]. In particular we will compute the matrix element in the modified minimal subtraction ($\overline{\text{MS}}$) scheme which is the standard reference scheme for comparing to experiment. However, as lattice measurements are carried out in a lattice motivated renormalization scheme known as the modified regularization invariant (RI') scheme [5,6], we will also produce the Green's function in that scheme. Equally we will determine the anomalous dimension of the tensor operator to four loops in both schemes. We qualify this by noting that the $\overline{\text{MS}}$ four loop tensor anomalous dimension is already available but only for the $SU(3)$ color group, [22]. We will provide the full four loop $\overline{\text{MS}}$ result for an arbitrary color group. Although lattice computations of operator Green's functions are invariably performed in the Landau gauge we will take a more general point of view and carry out our calculations in an arbitrary linear covariant gauge.

The paper is organized as follows. We recall the basic field theory formalism that allows us to compute the Green's function of interest with the tensor operator insertion in Sec. II. This includes the renormalization aspects and the definition of the RI' scheme. The focus of Sec. III is to record explicit four loop expressions and in particular the value of the Green's function as well as the $\overline{\text{MS}}$ operator anomalous dimension in both schemes. Concluding remarks are provided in Sec. IV while an appendix records expressions for an arbitrary linear covariant gauge and color group.

II. BACKGROUND

To begin with we define the Green's function that will be our focus which is

$$G_{\mathcal{O}^T}^{\mu\nu}(p) = \langle \psi(p) [\bar{\psi} \sigma^{\mu\nu} \psi](0) \bar{\psi}(-p) \rangle \quad (2.1)$$

where the tensor operator

$$\mathcal{O}^T = \bar{\psi} \sigma^{\mu\nu} \psi \quad (2.2)$$

is inserted at zero momentum and the antisymmetric tensor $\sigma^{\mu\nu}$ is defined by

$$\sigma^{\mu\nu} = \frac{1}{2} [\gamma^\mu, \gamma^\nu] \quad (2.3)$$

meaning that $G_{\mathcal{O}^T}^{\mu\nu}(p)$ is also antisymmetric. The first stage of determining the corrections to the Green's function is to decompose it into its Lorentz components which are formally defined by

$$G_{\mathcal{O}^T}^{\mu\nu}(p) = \Sigma_{\mathcal{O}^T}^{(1)}(p) \sigma^{\mu\nu} + \Sigma_{\mathcal{O}^T}^{(2)}(p) (\not{p} \gamma^\mu p^\nu - \not{p} \gamma^\nu p^\mu) \frac{1}{p^2} \quad (2.4)$$

where $\Sigma_{\mathcal{O}^T}^{(i)}(p)$ are scalar functions. These are isolated formally by a projection method [7]. Contracting the Green's function with two independent tensors produces a set of linear equations that can be inverted to deduce that

$$\begin{aligned} \Sigma_{\mathcal{O}^T}^{(1)}(p) &= -\frac{1}{4(d-1)(d-2)} \left[\text{tr} \left(\sigma_{\mu\nu} G_{\mathcal{O}^T}^{\mu\nu}(p) \right) \right. \\ &\quad \left. + \frac{1}{p^2} \text{tr} \left((\not{p} \gamma_\mu p_\nu - \not{p} \gamma_\nu p_\mu) G_{\mathcal{O}^T}^{\mu\nu}(p) \right) \right], \\ \Sigma_{\mathcal{O}^T}^{(2)}(p) &= -\frac{1}{4(d-1)(d-2)} \left[\text{tr} \left(\sigma_{\mu\nu} G_{\mathcal{O}^T}^{\mu\nu}(p) \right) \right. \\ &\quad \left. + \frac{d}{2p^2} \text{tr} \left((\not{p} \gamma_\mu p_\nu - \not{p} \gamma_\nu p_\mu) G_{\mathcal{O}^T}^{\mu\nu}(p) \right) \right] \quad (2.5) \end{aligned}$$

where the trace tr is over the spinor indices. This is carried out in d dimensions since we will be regularizing dimensionally in $d = 4 - 2\epsilon$ dimensions. At the outset we note that this is the same setup that was utilized in [7]. We have retained the same approach to allow those interested in extending their lattice matching analyses to readily adapt their programs to include the new perturbative corrections.

We now summarize the technical aspects of evaluating (2.1). The main reason for writing the amplitudes as linear combinations of two projections is to evaluate them by automatic Feynman graph integration packages. In [7] the three loop computations were carried out with the MINCER package that was originally devised and implemented in SCHOONSCHIP in [23] but recoded, [24], in the symbolic manipulation language FORM in [25,26]. The MINCER algorithm evaluates massless 2-point Feynman integrals in $d = 4 - 2\epsilon$ dimensions to three loops. Therefore as the operator \mathcal{O}^T is inserted at zero momentum then the package could be used to determine $G_{\mathcal{O}^T}^{\mu\nu}(p)$ to three loops.

To extend the results of [7] to the next order we follow the same approach but use the more recent FORCER package, [27,28]. This is the successor to MINCER in that it equally determines the ϵ expansion of 2-point massless Feynman integrals in d dimensions but at four loops. In order to effect the evaluation of (2.1) the first stage is to generate the Feynman graphs which is achieved by using the QGRAF package [29]. In addition to the 1, 13 and 244 graphs at respectively one, two and three loops, there are 5728 to determine at four loops. Once the graphs are generated the Lorentz and color indices are appended to the fields and the QCD Feynman rules implemented. To handle the group theory we used the `color.h` FORM module, based on the article [30], as it is designed to account for any new higher rank color Casimirs that will arise. This routine is applied to each graph in the automatic evaluation prior to applying the FORCER component as it can be the case that for certain graphs the group factor turns out to be zero. After the group factor is determined and the ϵ expansion found the expressions for each graph are added. To ensure that a finite value (2.1) is returned we carry out an automatic renormalization using the method of [31]. The key point is that the value of each graph is written as a function of the bare parameters. These are the gauge coupling constant g and the covariant gauge parameter α where the Landau gauge corresponds to a value of zero. We have chosen to include α since the operator anomalous dimension is independent of the parameter in the $\overline{\text{MS}}$ scheme, [32,33], and this property can be exploited for checking purposes. However this property does not persist in other schemes such as RI'. To introduce counterterms to render (2.1) finite the bare parameters are replaced by their renormalized partners. As the coupling and gauge parameter first occur in the one loop graph their renormalization constants are

only required at three loops. The overall divergence that remains in the Green's function after completing this process is then absorbed by the operator renormalization constant at four loops in whichever renormalization scheme is required.

There is one caveat to this in that the four loop quark wave function renormalization constant has to be included due to the external legs of (2.1). This and the other field wave function renormalization constants are now available to *five* loops in the $\overline{\text{MS}}$ scheme. For the extension of the three loop RI' tensor operator anomalous dimension we also need the quark wave function renormalization in that scheme but now at four loops. Therefore we have separately renormalized the quark 2-point function at four loops using FORCER which involved the evaluation of 1422 graphs at that order. We obtained the same four loop $\overline{\text{MS}}$ expression for the quark anomalous dimension $\gamma_\psi(a, \alpha)$ as [34–36] where $a = g^2/(16\pi^2)$. However it is a straightforward exercise to determine the anomalous dimension in the RI' scheme which is defined by the criterion given in [5,6] which is

$$\lim_{\epsilon \rightarrow 0} \left[Z_\psi^{\text{RI}'} \Sigma_\psi(p) \right] \Big|_{p^2=\mu^2} = \not{p} \quad (2.6)$$

at the subtraction point where $\Sigma_\psi(p)$ is the quark 2-point function and μ is a mass scale necessary in the regularization to ensure the coupling constant remains dimensionless in d dimensions. In other words at the subtraction point there are no $O(a)$ corrections to $\Sigma_\psi(p)$. With this definition we verified the three loop RI' expression of [7,37] for $\gamma_\psi(a, \alpha)$ and deduced

$$\begin{aligned} \gamma_\psi^{\text{RI}'}(a, 0) \Big|^{SU(3)} &= -[4N_f - 67] \frac{a^2}{3} + [416N_f^2 + 1728\zeta_3 N_f - 17888N_f - 32778\zeta_3 + 156963] \frac{a^3}{108} \\ &\quad - [16000N_f^3 + 103680\zeta_3 N_f^2 - 1205680N_f^2 - 5834784\zeta_3 N_f + 1075680\zeta_5 N_f \\ &\quad + 24606080N_f + 62524516\zeta_3 - 15846715\zeta_5 - 143460448] \frac{a^4}{1296} \\ &\quad + O(a^5) \end{aligned} \quad (2.7)$$

at four loops for $SU(3)$ or

$$\begin{aligned} \gamma_\psi^{\text{RI}'}(a, 0) \Big|^{SU(3)} &= -[1.333333N_f - 22.333333]a^2 \\ &\quad + [3.851852N_f^2 - 146.396719N_f + 1088.536841]a^3 \\ &\quad - [12.345679N_f^3 - 834.144090N_f^2 + 14434.984616N_f - 65381.420167]a^4 \\ &\quad + O(a^5) \end{aligned} \quad (2.8)$$

numerically.

III. TENSOR CURRENT RESULTS

Having described the computational technicalities we now record the results relating to (2.1). First we recall the result of [22] for the renormalization of the tensor current in the $\overline{\text{MS}}$ scheme for $SU(3)$ is

$$\begin{aligned} \gamma_T^{\overline{\text{MS}}}(a) \Big|^{SU(3)} &= \frac{4}{3}a + \frac{2}{27}[543 - 26N_f]a^2 \\ &+ [52555 - 36N_f^2 - 1440\zeta_3 N_f - 5240N_f - 2784\zeta_3] \frac{a^3}{81} \\ &+ [1152\zeta_3 N_f^3 + 168N_f^3 + 66240\zeta_3 N_f^2 - 25920\zeta_4 N_f^2 + 39844N_f^2 \\ &- 1821984\zeta_3 N_f + 377568\zeta_4 N_f + 993600\zeta_5 N_f - 3074758N_f \\ &- 742368\zeta_3 + 826848\zeta_4 - 4018560\zeta_5 + 19876653] \frac{a^4}{1458} + O(a^5). \end{aligned} \quad (3.1)$$

We have verified this as a corollary of the expression for an arbitrary color group which is

$$\begin{aligned} \gamma_T^{\overline{\text{MS}}}(a) &= C_F a + \left[\frac{257}{18} C_F C_A - \frac{26}{9} C_F T_F N_f - \frac{19}{2} C_F^2 \right] a^2 \\ &+ \left[\left[\frac{13639}{108} - 40\zeta_3 \right] C_F C_A^2 - \frac{4}{3} C_F T_F^2 N_f^2 - \left[\frac{1004}{27} + 16\zeta_3 \right] C_F C_A T_F N_f \right. \\ &+ \left. \left[\frac{98}{9} + 16\zeta_3 \right] C_F^2 T_F N_f + \left[112\zeta_3 - \frac{6823}{36} \right] C_F^2 C_A + \left[\frac{365}{6} - 64\zeta_3 \right] C_F^3 \right] a^3 \\ &+ \left[\left[\frac{208}{3} \zeta_3 - \frac{32}{3} - \frac{640}{3} \zeta_5 \right] \frac{d_F^{abcd} d_A^{abcd}}{N_F} + [128 - 32\zeta_3] \frac{d_A^{abcd} d_A^{abcd}}{N_F} \right. \\ &+ \left. \left[\frac{56}{81} + \frac{128}{27} \zeta_3 \right] C_F T_F^3 N_f^3 + \left[\frac{194}{81} - 32\zeta_4 + \frac{736}{9} \zeta_3 \right] C_F C_A T_F^2 N_f^2 \right. \\ &+ \left. \left[8\zeta_4 - \frac{73409}{162} + \frac{400}{3} \zeta_5 - \frac{980}{3} \zeta_3 \right] C_F C_A^2 T_F N_f \right. \\ &+ \left. \left[\frac{710581}{648} - \frac{1600}{9} \zeta_5 + 220\zeta_4 - \frac{12598}{27} \zeta_3 \right] C_F C_A^3 \right. \\ &+ \left. \left[\frac{4544}{81} + 32\zeta_4 - \frac{736}{9} \zeta_3 \right] C_F^2 T_F^2 N_f^2 \right. \\ &+ \left. \left[\frac{523}{3} + \frac{80}{3} \zeta_5 + 136\zeta_4 + \frac{2416}{9} \zeta_3 \right] C_F^2 C_A T_F N_f \right. \\ &+ \left. \left[\frac{2320}{3} \zeta_5 - 616\zeta_4 + \frac{9800}{9} \zeta_3 - \frac{733979}{324} \right] C_F^2 C_A^2 \right. \\ &+ \left. \left[\frac{2900}{27} - 160\zeta_5 - 128\zeta_4 - \frac{8}{9} \zeta_3 \right] C_F^3 T_F N_f \right. \\ &+ \left. \left[\frac{179363}{108} - \frac{4880}{3} \zeta_5 + 352\zeta_4 + \frac{1012}{9} \zeta_3 \right] C_F^3 C_A \right. \\ &+ \left. \left[\frac{3200}{3} \zeta_5 - \frac{2000}{3} \zeta_3 - \frac{10489}{24} \right] C_F^4 \right] a^4 + O(a^5) \end{aligned} \quad (3.2)$$

where ζ_n is the Riemann zeta function and C_F , C_A and T_F are the standard color factors. At four loops the rank 4 color Casimirs d_R^{abcd} arise with the tensor being defined by

$$d_R^{abcd} = \frac{1}{6} \text{Tr}(T^a T^{(b} T^c T^{d)}) \quad (3.3)$$

for the representation R where the trace Tr is over the color indices of the matrices representing the group generators T^a . En route we have verified the earlier respective two and three loop terms derived in [38,39]. The three loop term had previously been confirmed in [40]. For practical purposes we recall the numerical value is [22]

$$\begin{aligned} \gamma_T^{\overline{\text{MS}}}(a) \Big|^{SU(3)} &= 1.333333a + [40.222222 - 1.925926N_f]a^2 \\ &+ [607.512019 - 86.061258N_f - 0.444444N_f^2]a^3 \\ &+ [1.065000N_f^3 + 62.698512N_f^2 - 2624.104532N_f + 10776.573952]a^4 \\ &+ O(a^5) \end{aligned} \quad (3.4)$$

for $SU(3)$.

While the $SU(3)$ value of $\gamma_T^{\overline{\text{MS}}}(a)$ was already available [22], what is one of the main results here is the extension of $\Sigma_{O^r}^{(1)}(p)$ to four loops. In particular we have

$$\begin{aligned} \Sigma_{O^r}^{(1)\overline{\text{MS}}}(p) \Big|_{\alpha=0}^{SU(3)} &= 1 + \left[\frac{76}{9} \zeta_3 - \frac{1693}{54} + \frac{124}{81} N_f \right] a^2 \\ &+ \left[\frac{22952}{243} \zeta_3 - \frac{277}{108} \zeta_4 - \frac{265}{81} \zeta_5 - \frac{1977125}{2916} \right. \\ &+ \left. \left[\frac{63764}{729} + \frac{80}{9} \zeta_4 - \frac{776}{27} \zeta_3 \right] N_f + \left[\frac{376}{2187} - \frac{32}{81} \zeta_3 \right] N_f^2 \right] a^3 \\ &+ \left[\frac{42157925}{31104} \zeta_6 - \frac{629370181}{23328} - \frac{476917595}{15552} \zeta_7 + \frac{2784917789}{46656} \zeta_5 \right. \\ &- \left. \frac{1202905}{2592} \zeta_4 - \frac{538028059}{23328} \zeta_3 + \frac{48310147}{15552} \zeta_3^2 \right. \\ &+ \left. \left[\frac{124447867}{17496} + \frac{2989}{2} \zeta_7 - \frac{12400}{27} \zeta_6 - \frac{5255677}{972} \zeta_5 + \frac{283045}{648} \zeta_4 \right. \right. \\ &+ \left. \left. \frac{1452433}{972} \zeta_3 - \frac{1880}{9} \zeta_3^2 \right] N_f \right. \\ &+ \left. \left[\frac{3320}{27} \zeta_5 - \frac{280}{27} \zeta_4 - \frac{2548}{81} \zeta_3 - \frac{13603319}{52488} \right] N_f^2 \right. \\ &+ \left. \left[\frac{4610}{6561} - \frac{8}{27} \zeta_4 + \frac{32}{243} \zeta_3 \right] N_f^3 \right] a^4 + O(a^5) \end{aligned} \quad (3.5)$$

in the Landau gauge at the subtraction point and

$$\Sigma_{O^r}^{(2)\overline{\text{MS}}}(p) \Big|_{\alpha=0}^{SU(3)} = 0 \quad (3.6)$$

for $SU(3)$ with

$$\begin{aligned} \Sigma_{O^r}^{(1)\overline{\text{MS}}}(p) \Big|_{\alpha=0}^{SU(3)} &= 1 + [1.530864N_f - 0.277778\alpha^2 - 2.424683\alpha - 21.201149]a^2 \\ &+ [62.540409N_f - 1.046804\alpha^3 - 17.386077\alpha^2 - 5.043485\alpha N_f \\ &- 10.680631\alpha - 0.302962N_f^2 - 570.657293]a^3 \\ &+ [11.928069\alpha^2 N_f - 9.031353\alpha^4 - 118.197512\alpha^3 - 527.617841\alpha^2 \\ &- 3.840997\alpha N_f^2 + 155.224548\alpha N_f - 1864.356282\alpha + 0.540244N_f^3 \\ &- 180.703312N_f^2 + 4513.065131N_f - 18365.189753]a^4 \\ &+ O(a^5) \end{aligned} \quad (3.7)$$

numerically for the nonzero amplitude. We note as was observed before [7,22], the value of the channel 2 amplitude is zero at four loops not only for $SU(3)$ but also for a general color group. This may in fact be true to all orders as a consequence of some symmetry restriction. We have recorded the full four loop expression for $\Sigma_{\mathcal{O}^r}^{(1)\overline{\text{MS}}}(p)$ in the Appendix and provided its electronic representation in the associated data file together with other results relating to the tensor operator. To gauge the effect of the new correction when $N_f = 3$ we have

$$\Sigma_{\mathcal{O}^r}^{(1)\overline{\text{MS}}}(p) \Big|_{\alpha=0}^{SU(3)N_f=3} = 1 - 16.608556a^2 - 385.762720a^3 - 6437.737582a^4 + O(a^5) \quad (3.8)$$

and with $\alpha_s = 0.12$ its two, three and four loop values are 0.998486, 0.998150 and 0.998096 respectively using naive substitution. Viewed this way one would imagine that the imperceptible difference between the three and four loop results could lead to a minor refinement of the error on the lattice extrapolation to the high energy expression. This observation is one of the main consequences of our next order study. At this point we note that we found a discrepancy in the N_f independent part of the three loop term

of $\Sigma_{\mathcal{O}^r}^{(1)\overline{\text{MS}}}(p)$ given in [7]. In particular it has only a minor effect in the $O(a^3)$ coefficient. For example evaluating the corresponding $O(a^3)$ coefficient of (3.8) in [7] at $N_f = 3$ in the Landau gauge would have given -399.155300 . With this value then at three loops (3.8) evaluates to 0.998084 at $\alpha_s = 0.12$ so that there is no large discrepancy.

The focus so far has been on the $\overline{\text{MS}}$ scheme but in [7] the operator was also renormalized in the RI' scheme. For completeness we also extend the three loop results for that scheme here. First we recall the definition of the operator renormalization constant of [7], that has parallels with the quark wave function renormalization definition of (2.6), which is

$$\lim_{\epsilon \rightarrow 0} \left[Z_{\psi}^{\text{RI}'} Z_{\mathcal{O}^r}^{\text{RI}'} \Sigma_{\mathcal{O}^r}^{(1)}(p) \right] \Big|_{p^2=\mu^2} = 1. \quad (3.9)$$

In other words the channel 1 amplitude is used since the divergences that lead to the $\overline{\text{MS}}$ scheme renormalization are located there irrespective of the fact that $\Sigma_{\mathcal{O}^r}^{(2)}(p)$ vanishes. With (3.9) the anomalous dimension RI' scheme anomalous dimension $\gamma_{\mathcal{O}^r}^{\text{RI}'}(a, \alpha)$ is

$$\begin{aligned} \gamma_{\mathcal{O}^r}^{\text{RI}'}(a, 0) = & C_F a + C_F [257C_A - 171C_F - 52N_f T_F] \frac{C_A a^2}{18} \\ & + [53387C_A^2 - 23112\zeta_3 C_A^2 + 41904\zeta_3 C_A C_F - 57186C_A C_F + 3456\zeta_3 C_A N_f T_F \\ & - 24884C_A N_f T_F - 10368\zeta_3 C_F^2 + 9855C_F^2 - 6048\zeta_3 C_F N_f T_F \\ & + 11394C_F N_f T_F + 2288N_f^2 T_F^2] \frac{C_F a^3}{162} \\ & + [97637317C_A^3 C_F N_F + 5196960\zeta_5 C_A^3 C_F N_F - 57962790\zeta_3 C_A^3 C_F N_F \\ & + 103267872\zeta_3 C_A^2 C_F^2 N_F + 1321920\zeta_5 C_A^2 C_F^2 N_F - 135883278C_A^2 C_F^2 N_F \\ & + 26573832\zeta_3 C_A^2 C_F N_F N_f T_F - 1088640\zeta_5 C_A^2 C_F N_F N_f T_F \\ & - 72145932C_A^2 C_F N_F N_f T_F - 20785248\zeta_3 C_A C_F^3 N_F \\ & - 17262720\zeta_5 C_A C_F^3 N_F + 43519680C_A C_F^3 N_F - 42000768\zeta_3 C_A C_F^2 N_F N_f T_F \\ & + 3110400\zeta_5 C_A C_F^2 N_F N_f T_F + 57759192C_A C_F^2 N_F N_f T_F \\ & - 2695680\zeta_3 C_A C_F N_F N_f^2 T_F^2 + 15287808C_A C_F N_F N_f^2 T_F^2 - 7776000\zeta_3 C_F^4 N_F \\ & + 12441600\zeta_5 C_F^4 N_F - 5097654C_F^4 N_F + 6158592\zeta_3 C_F^3 N_F N_f T_F \\ & - 2488320\zeta_5 C_F^3 N_F N_f T_F - 5448384C_F^3 N_F N_f T_F + 3525120\zeta_3 \zeta_5 C_F^2 N_F N_f^2 T_F^2 \\ & - 5053824C_F^2 N_F N_f^2 T_F^2 - 872192C_F N_F N_f^3 T_F^3 + 808704\zeta_3 d_F^{abcd} d_A^{abcd} \\ & - 2488320\zeta_5 d_F^{abcd} d_A^{abcd} - 124416d_F^{abcd} d_A^{abcd} - 373248\zeta_3 d_F^{abcd} d_F^{abcd} N_f \\ & + 1492992d_F^{abcd} d_F^{abcd} N_f] \frac{a^4}{11664N_F} + O(a^5) \end{aligned} \quad (3.10)$$

in the Landau gauge. Although the tensor operator is gauge invariant its anomalous dimension will be dependent on the gauge parameter in general. It is only in the $\overline{\text{MS}}$ scheme that the anomalous dimension of a gauge invariant operator is

independent of the gauge parameter, [32,33]. Indeed that was a check on the emergence of an α independent $\overline{\text{MS}}$ expression at four loops for a general color group. For comparison we note

$$\begin{aligned} \gamma_{\mathcal{O}^r}^{\text{RI}'}(a, 0)|^{SU(3)} &= 1.333333a + [40.222222 - 1.925926N_f]a^2 \\ &+ [4.707819N_f^2 - 233.294078N_f + 1634.149833]a^3 \\ &+ [88297.353564 - 18912.306371N_f + 1001.765247N_f^2 \\ &- 12.462734N_f^3]a^4 + O(a^5) \end{aligned} \quad (3.11)$$

numerically. We do not need to record the RI' expression for $\Sigma_{\mathcal{O}^r}^{(1)}(p)$ as trivially it will be unity by construction.

One check on our four loop RI' tensor operator anomalous dimension is to exploit a useful property of the renormalization group formalism. If an anomalous dimension is known at L loops in one renormalization scheme and has been renormalized to $(L - 1)$ loops in another scheme one can deduce the L loop anomalous dimension in the latter scheme by using a conversion function. This is defined as the ratio of the renormalization constants in the respective schemes at $(L - 1)$ loops. In our particular case the conversion function $C_{\mathcal{O}^r}(a, \alpha)$ is defined by

$$C_{\mathcal{O}^r}(a, \alpha) = \frac{Z_{\mathcal{O}^r}^{\text{RI}'}}{Z_{\mathcal{O}^r}^{\overline{\text{MS}}}} \quad (3.12)$$

where the variables of the argument are in the $\overline{\text{MS}}$ scheme. We note this since $Z_{\mathcal{O}^r}^{\text{RI}'}$ is a function of $a^{\text{RI}'}$ and $\alpha^{\text{RI}'}$ which would suggest that $C_{\mathcal{O}^r}(a, \alpha)$ is not dependent on ϵ but also has poles in the regularization. This is not the case since $a^{\text{RI}'}$ and $\alpha^{\text{RI}'}$ are functions of $a^{\overline{\text{MS}}}$ and $\alpha^{\overline{\text{MS}}}$ with the relation between the two sets being established to three loops in [7]. Strictly only the relation of the gauge parameters is needed to this order since the coupling constants are the same in both schemes. In [7] the three loop terms of the gauge parameter map were actually superfluous for the three loop check analogous to the one we will repeat here but

are needed at four loops. Once $C_{\mathcal{O}^r}(a, \alpha)$ is available the anomalous dimensions between the two schemes are connected by

$$\begin{aligned} \gamma_{\mathcal{O}^r}^{\text{RI}'}(a_{\text{RI}'}, \alpha_{\text{RI}'}) &= \left[\gamma_{\mathcal{O}^r}^{\overline{\text{MS}}}(a_{\overline{\text{MS}}}) - \beta(a_{\overline{\text{MS}}}) \frac{\partial}{\partial a_{\overline{\text{MS}}}} \ln C_{\mathcal{O}^r}(a_{\overline{\text{MS}}}, \alpha_{\overline{\text{MS}}}) \right. \\ &\left. - \alpha_{\overline{\text{MS}}} \gamma_{\alpha}^{\overline{\text{MS}}}(a_{\overline{\text{MS}}}, \alpha_{\overline{\text{MS}}}) \frac{\partial}{\partial \alpha_{\overline{\text{MS}}}} \ln C_{\mathcal{O}^r}(a_{\overline{\text{MS}}}, \alpha_{\overline{\text{MS}}}) \right]_{\overline{\text{MS}} \rightarrow \text{RI}'} \end{aligned} \quad (3.13)$$

We have labeled the variables in the two different schemes explicitly for clarity. As the right hand side of (3.13) involves variables in the $\overline{\text{MS}}$ scheme these have to be mapped to their RI' counterparts which is the meaning of the restriction on the right square bracket. It is a simple exercise to infer $\alpha_{\overline{\text{MS}}}(a_{\text{RI}'}, \alpha_{\text{RI}'})$ from the three loop expression of $\alpha_{\text{RI}'}(a_{\overline{\text{MS}}}, \alpha_{\overline{\text{MS}}})$ given in [7] to facilitate this. We have recorded the *four* loop Landau gauge expression for $C_{\mathcal{O}^r}(a, \alpha)$ for a general color group in the Appendix with the full arbitrary gauge expression given in the attached data file. While the four loop term is not needed to carry out the check of (3.10) given (3.2) it will in fact be useful once the five loop $\overline{\text{MS}}$ expression for (3.2) is available. As a point of reference we note

$$\begin{aligned} C_{\mathcal{O}^r}(a, 0)|^{SU(3)} &= 1 + [46.665355 - 3.864197N_f]a^2 \\ &+ [6.763867N_f^2 - 308.983059N_f + 2060.637793]a^3 \\ &+ [97451.822851 - 23266.484197N_f + 1309.625138N_f^2 \\ &- 15.567877N_f^3]a^4 + O(a^5) \end{aligned} \quad (3.14)$$

numerically. Finally we record that using (3.13) we reproduced (3.10) precisely for an arbitrary color group and gauge parameter.

IV. DISCUSSION

We have evaluated the Green's function with the quark bilinear tensor operator inserted in a quark 2-point function to four loops in QCD for both the $\overline{\text{MS}}$ and the lattice motivated RI' renormalization schemes. As a corollary we have deduced the tensor operator anomalous dimension in the $\overline{\text{MS}}$ scheme for an arbitrary color group. To gain an insight into the effect of the new loop order we have shown that for $SU(3)$ and three quark flavors the four loop correction of the Green's function in the Landau gauge represents a insignificantly small difference to the three loop value at the same benchmark point in the $\overline{\text{MS}}$ scheme. While this is not unrelated to the fact that the one loop correction for this Green's function is zero in the Landau gauge it perhaps indicates that any error on the lattice extrapolation to the high energy continuum value could be very well under control for this particular operator. One obvious test of this would be for a reexamination of

previous lattice extrapolations to the high energy limit but using the new four loop perturbative results rather than the previous three loop ones.

The data representing the main results here are accessible from [41].

ACKNOWLEDGMENTS

This work was carried out with the support of the STFC Consolidated Grant ST/T000988/1 and partly with the support of a DFG Mercator Fellowship.

APPENDIX: RESULTS FOR GENERAL COLOR GROUP

As the four loop expressions for an arbitrary color group are large we record them here for completeness. First, the $\overline{\text{MS}}$ nonzero amplitude is

$$\begin{aligned}
\Sigma_{Or}^{(1)\overline{\text{MS}}}(p) = & 1 + \left[\left[11\zeta_3 - \frac{3773}{216} + 3\alpha - 3\zeta_3\alpha + \frac{3}{8}\alpha^2 \right] C_F C_A + \left[\frac{65}{3} - 20\zeta_3 - \alpha^2 \right] C_F^2 \right. \\
& + \left. \frac{62}{27} N_f T_F C_F \right] a^2 \\
& + \left[\left[\frac{251}{16}\zeta_4 - \frac{4180535}{11664} - \frac{185}{12}\zeta_5 + \frac{6742}{27}\zeta_3 + \frac{12817}{576}\alpha + \frac{35}{6}\zeta_5\alpha + \frac{3}{8}\zeta_4\alpha \right. \right. \\
& - \left. \frac{253}{12}\zeta_3\alpha + \frac{197}{64}\alpha^2 + \frac{5}{4}\zeta_5\alpha^2 + \frac{3}{16}\zeta_4\alpha^2 - \frac{15}{4}\zeta_3\alpha^2 + \frac{29}{48}\alpha^3 - \frac{1}{3}\zeta_3\alpha^3 \right] C_F C_A^2 \\
& + \left[\frac{62018}{81} + 40\zeta_5 - 50\zeta_4 - \frac{1862}{3}\zeta_3 - \frac{1}{6}\alpha + 20\alpha\zeta_5 - \frac{79}{3}\zeta_3\alpha - 6\alpha^2 + 2\zeta_3\alpha^2 \right. \\
& - \left. \frac{3}{2}\alpha^3 + \zeta_3\alpha^3 \right] C_F^2 C_A + \left[32\zeta_4 - \frac{5246}{27} - \frac{40}{3}\zeta_5 + \frac{1550}{9}\zeta_3 + \alpha + 2\zeta_3\alpha - 2\alpha^2 + 2\zeta_3\alpha^2 - \frac{2}{3}\zeta_3\alpha^3 \right] C_F^3 \\
& + \left[\frac{79544}{729} + 8\zeta_4 - \frac{1732}{27}\zeta_3 - \frac{673}{72}\alpha + 4\zeta_3\alpha \right] N_f T_F C_F C_A \\
& + \left[112\zeta_3 - \frac{23831}{162} - 8\zeta_4 + \frac{4}{3}\alpha + \frac{8}{3}\zeta_3\alpha \right] N_f T_F C_F^2 \\
& + \left[\frac{376}{729} - \frac{32}{27}\zeta_3 \right] N_f^2 T_F^2 C_F \right] a^3 \\
& + \left[\left[\frac{1568515}{288}\zeta_5 - \frac{3403}{18} - \frac{282737}{48}\zeta_7 + \frac{12775}{192}\zeta_6 + \frac{1675}{64}\zeta_4 - \frac{119405}{144}\zeta_3 \right. \right. \\
& + \frac{136595}{96}\zeta_3^2 + \frac{23}{6}\alpha + \frac{1939}{96}\zeta_7\alpha - \frac{275}{8}\zeta_6\alpha - \frac{1415}{6}\zeta_5\alpha + \frac{303}{16}\zeta_4\alpha + \frac{429}{2}\zeta_3\alpha \\
& + \frac{1}{4}\zeta_3^2\alpha + \frac{259}{8}\zeta_7\alpha^2 - \frac{175}{32}\zeta_6\alpha^2 - \frac{475}{16}\zeta_5\alpha^2 + \frac{33}{32}\zeta_4\alpha^2 - \frac{65}{24}\zeta_3\alpha^2 + \frac{53}{16}\zeta_3^2\alpha^2 \\
& + \frac{441}{32}\zeta_7\alpha^3 - \frac{15}{2}\zeta_5\alpha^3 - \frac{9}{16}\zeta_4\alpha^3 - \frac{5}{2}\zeta_3\alpha^3 - 3\zeta_3^2\alpha^3 + \frac{25}{64}\zeta_6\alpha^4 + \frac{75}{32}\zeta_5\alpha^4 \\
& - \left. \frac{21}{64}\zeta_4\alpha^4 - \frac{21}{16}\zeta_3\alpha^4 - \frac{19}{32}\zeta_3^2\alpha^4 \right] \frac{d_F^{abcd} d_A^{abcd}}{N_F}
\end{aligned}$$

$$\begin{aligned}
 & + \left[\frac{69475}{2304} \zeta_6 - \frac{2408522491}{279936} - \frac{2520203}{2304} \zeta_7 + \frac{1622471}{1152} \zeta_5 + \frac{638629}{4608} \zeta_4 \right. \\
 & + \frac{30933595}{5184} \zeta_3 + \frac{96271}{576} \zeta_3^2 + \frac{232652657}{746496} \alpha - \frac{18067}{576} \zeta_7 \alpha - \frac{2875}{192} \zeta_6 \alpha \\
 & + \frac{217739}{1728} \zeta_5 \alpha + \frac{2727}{256} \zeta_4 \alpha - \frac{173347}{432} \zeta_3 \alpha + \frac{1999}{32} \zeta_3^2 \alpha + \frac{1028105}{27648} \alpha^2 \\
 & + \frac{847}{768} \zeta_7 \alpha^2 - \frac{475}{384} \zeta_6 \alpha^2 + \frac{2309}{144} \zeta_5 \alpha^2 + \frac{567}{256} \zeta_4 \alpha^2 - \frac{49489}{1152} \zeta_3 \alpha^2 - \frac{197}{96} \zeta_3^2 \alpha^2 \\
 & + \frac{13777}{1536} \alpha^3 + \frac{147}{128} \zeta_7 \alpha^3 + \frac{73}{64} \zeta_5 \alpha^3 + \frac{63}{256} \zeta_4 \alpha^3 - \frac{97}{12} \zeta_3 \alpha^3 - \frac{1}{16} \zeta_3^2 \alpha^3 \\
 & \left. + \frac{529}{384} \alpha^4 + \frac{25}{768} \zeta_6 \alpha^4 + \frac{5}{128} \zeta_5 \alpha^4 + \frac{1}{512} \zeta_4 \alpha^4 - \frac{199}{384} \zeta_3 \alpha^4 - \frac{5}{192} \zeta_3^2 \alpha^4 \right] C_F C_A^3 \\
 & + \left[\frac{2009482489}{93312} + \frac{521633}{96} \zeta_7 + \frac{175}{24} \zeta_6 - \frac{25435}{18} \zeta_5 - \frac{23389}{48} \zeta_4 - \frac{4088551}{216} \zeta_3 \right. \\
 & - \frac{15779}{12} \zeta_3^2 + \frac{27239}{432} \alpha - \frac{791}{12} \zeta_7 \alpha + \frac{25}{8} \zeta_6 \alpha + \frac{55}{9} \zeta_5 \alpha - \frac{21}{16} \zeta_4 \alpha - \frac{25519}{216} \zeta_3 \alpha \\
 & - \frac{103}{4} \zeta_3^2 \alpha - \frac{42625}{576} \alpha^2 - \frac{427}{32} \zeta_7 \alpha^2 + \frac{85}{4} \zeta_5 \alpha^2 + \frac{1315}{72} \zeta_3 \alpha^2 + \frac{9}{2} \zeta_3^2 \alpha^2 \\
 & \left. - \frac{313}{16} \alpha^3 + \frac{57}{8} \zeta_3 \alpha^3 - \frac{495}{128} \alpha^4 + \frac{5}{4} \zeta_3 \alpha^4 \right] C_F^2 C_A^2 \\
 & + \left[\frac{350}{3} \zeta_6 - \frac{224041}{24} - \frac{71113}{6} \zeta_7 + \frac{42629}{9} \zeta_5 + \frac{1655}{6} \zeta_4 + \frac{89683}{9} \zeta_3 + \frac{7100}{3} \zeta_3^2 \right. \\
 & - \frac{313}{3} \alpha - \frac{105}{2} \zeta_7 \alpha + \frac{530}{3} \zeta_5 \alpha - \frac{20}{9} \zeta_3 \alpha + 20 \zeta_3^2 \alpha - \frac{3533}{108} \alpha^2 + \frac{505}{18} \zeta_3 \alpha^2 \\
 & \left. - 5 \alpha^3 + 4 \zeta_3 \alpha^3 + \frac{5}{8} \alpha^4 - \frac{1}{2} \zeta_3 \alpha^4 \right] C_F^3 C_A \\
 & + \left[\frac{57551}{36} + \frac{19726}{3} \zeta_7 - \frac{800}{3} \zeta_6 - \frac{44710}{9} \zeta_5 + 100 \zeta_4 - \frac{10856}{9} \zeta_3 - \frac{2144}{3} \zeta_3^2 \right. \\
 & \left. + 41 \alpha - 44 \zeta_3 \alpha - \frac{8}{3} \alpha^2 + 4 \zeta_3 \alpha^2 \right] C_F^4 \\
 & + \left[1764 \zeta_7 - \frac{392}{3} - 1920 \zeta_5 + 12 \zeta_4 + \frac{4936}{3} \zeta_3 - 1216 \zeta_3^2 \right] N_f \frac{d_F^{abcd} d_F^{abcd}}{N_F} \\
 & + \left[\frac{59341063}{11664} - \frac{735}{4} \zeta_7 - \frac{400}{3} \zeta_6 - \frac{295943}{216} \zeta_5 + \frac{1951}{16} \zeta_4 - \frac{435797}{216} \zeta_3 - 236 \zeta_3^2 \right. \\
 & - \frac{18122533}{93312} \alpha + \frac{4081}{54} \zeta_5 \alpha - \frac{111}{8} \zeta_4 \alpha + \frac{656}{9} \zeta_3 \alpha + \frac{50}{3} \zeta_3^2 \alpha - \frac{16801}{1728} \alpha^2 \\
 & \left. - \frac{29}{72} \zeta_5 \alpha^2 - \frac{7}{16} \zeta_4 \alpha^2 + \frac{337}{72} \zeta_3 \alpha^2 + \zeta_3^2 \alpha^2 \right] N_f T_F C_F C_A^2 \\
 & + \left[882 \zeta_7 - \frac{107169125}{11664} + \frac{250}{3} \zeta_6 + \frac{9674}{9} \zeta_5 - \frac{302}{3} \zeta_4 + \frac{139813}{27} \zeta_3 + 868 \zeta_3^2 \right. \\
 & - \frac{99637}{864} \alpha - \frac{494}{9} \zeta_5 \alpha + \frac{33}{2} \zeta_4 \alpha + \frac{6905}{27} \zeta_3 \alpha - 32 \zeta_3^2 \alpha + \frac{965}{36} \alpha^2 \\
 & \left. - \frac{112}{9} \zeta_3 \alpha^2 \right] N_f T_F C_F^2 C_A
 \end{aligned}$$

$$\begin{aligned}
& + \left[\frac{67265}{72} + 100\zeta_6 + \frac{1624}{9}\zeta_5 - \frac{71}{3}\zeta_4 - \frac{3322}{9}\zeta_3 - 792\zeta_3^2 + \frac{476}{9}\alpha - \frac{488}{9}\zeta_3\alpha \right. \\
& \quad \left. + \frac{94}{27}\alpha^2 - \frac{16}{9}\zeta_3\alpha^2 \right] N_f T_F C_F^3 \\
& + \left[\frac{6328}{27}\zeta_5 - \frac{3806959}{5832} - \frac{56}{3}\zeta_4 + \frac{580}{3}\zeta_3 + \frac{35311}{1458}\alpha - \frac{80}{3}\zeta_5\alpha + 2\zeta_4\alpha \right. \\
& \quad \left. + \frac{76}{27}\zeta_3\alpha \right] N_f^2 T_F^2 C_F C_A \\
& + \left[\frac{1291207}{1458} - \frac{752}{3}\zeta_5 + \frac{56}{3}\zeta_4 - \frac{4552}{9}\zeta_3 - \frac{208}{27}\alpha - \frac{128}{27}\zeta_3\alpha \right] N_f^2 T_F^2 C_F^2 \\
& + \left[\frac{9220}{2187} - \frac{16}{9}\zeta_4 + \frac{64}{81}\zeta_3 \right] N_f^3 T_F^3 C_F \Big] a^4 + O(a^5). \tag{A1}
\end{aligned}$$

The conversion function for the tensor operator from the $\overline{\text{MS}}$ scheme to the RI' one in the Landau gauge is

$$\begin{aligned}
C_{OT}(a, 0) = & 1 + [5987C_A - 3024\zeta_3C_A + 4320\zeta_3C_F - 4815C_F - 1252N_fT_F] \frac{C_A a^2}{216} \\
& + [660960\zeta_5C_A^2 - 233280\zeta_4C_A^2 - 4438098\zeta_3C_A^2 + 7047161C_A^2 + 7752672\zeta_3C_A C_F \\
& \quad + 653184\zeta_4C_A C_F - 699840\zeta_5C_A C_F - 9415134C_A C_F + 950400\zeta_3C_A N_f T_F \\
& \quad - 93312\zeta_4C_A N_f T_F - 2984432C_A N_f T_F - 2008800\zeta_3C_F^2 - 373248\zeta_4C_F^2 \\
& \quad + 155520\zeta_5C_F^2 + 2195316C_F^2 - 1119744\zeta_3C_F N_f T_F + 93312\zeta_4C_F N_f T_F \\
& \quad + 1562256C_F N_f T_F + 13824\zeta_3N_f^2 T_F^2 + 220064N_f^2 T_F^2] \frac{C_F a^3}{11664} \\
& + \left[859248\zeta_3^2 C_A^3 C_F - 5427947484\zeta_3 C_A^3 C_F - 97962048\zeta_4 C_A^3 C_F \right. \\
& \quad + 307910160\zeta_5 C_A^3 C_F - 62208000\zeta_6 C_A^3 C_F + 226816443\zeta_7 C_A^3 C_F \\
& \quad + 7769141516C_A^3 C_F + 773276544\zeta_3^2 C_A^2 C_F^2 + 9867578112\zeta_3 C_A^2 C_F^2 \\
& \quad + 228614400\zeta_4 C_A^2 C_F^2 + 907933536\zeta_5 C_A^2 C_F^2 + 270604800\zeta_6 C_A^2 C_F^2 \\
& \quad - 2066061816\zeta_7 C_A^2 C_F^2 - 12614153610C_A^2 C_F^2 + 179159040\zeta_3^2 C_A^2 C_F N_f T_F \\
& \quad + 2217673728\zeta_3 C_A^2 C_F N_f T_F - 68584320\zeta_4 C_A^2 C_F N_f T_F \\
& \quad + 271216512\zeta_5 C_A^2 C_F N_f T_F + 46656000\zeta_6 C_A^2 C_F N_f T_F \\
& \quad - 20575296\zeta_7 C_A^2 C_F N_f T_F - 5293901856C_A^2 C_F N_f T_F - 1517626368\zeta_3^2 C_A C_F^3 \\
& \quad - 2501316288\zeta_3 C_A C_F^3 + 23607936\zeta_4 C_A C_F^3 - 2880479232\zeta_5 C_A C_F^3 \\
& \quad - 569203200\zeta_6 C_A C_F^3 + 3784548096\zeta_7 C_A C_F^3 + 5214521988C_A C_F^3 \\
& \quad - 575548416\zeta_3^2 C_A C_F^2 N_f T_F - 2772776448\zeta_3 C_A C_F^2 N_f T_F \\
& \quad + 56360448\zeta_4 C_A C_F^2 N_f T_F - 535735296\zeta_5 C_A C_F^2 N_f T_F \\
& \quad + 9331200\zeta_6 C_A C_F^2 N_f T_F + 4472230512C_A C_F^2 N_f T_F \\
& \quad - 160496640\zeta_3 C_A C_F N_f^2 T_F^2 + 17169408\zeta_4 C_A C_F N_f^2 T_F^2 \\
& \quad - 103845888\zeta_5 C_A C_F N_f^2 T_F^2 + 1012343136C_A C_F N_f^2 T_F^2 \\
& \quad + 579280896\zeta_3^2 C_F^4 - 905561856\zeta_3 C_F^4 - 139968000\zeta_4 C_F^4 \\
& \quad \left. + 2238243840\zeta_5 C_F^4 + 373248000\zeta_6 C_F^4 - 812464182C_F^4 \right]
\end{aligned}$$

$$\begin{aligned}
 & + 443418624\zeta_3^2 C_F^3 N_f T_F + 58371840\zeta_3 C_F^3 N_f T_F - 186624\zeta_4 C_F^3 N_f T_F \\
 & - 97293312\zeta_5 C_F^3 N_f T_F - 55987200\zeta_6 C_F^3 N_f T_F - 339420240 C_F^3 N_f T_F \\
 & + 134618112\zeta_3 C_F^2 N_f^2 T_F^2 - 17169408\zeta_4 C_F^2 N_f^2 T_F^2 + 140341248\zeta_5 C_F^2 N_f^2 T_F^2 \\
 & - 282227232 C_F^2 N_f^2 T_F^2 - 1437696\zeta_3 C_F N_f^3 T_F^3 + 995328\zeta_4 C_F N_f^3 T_F^3 \\
 & - 51645184 C_F N_f^3 T_F^3 - 710384256\zeta_3^2 \frac{d_F^{abcd} d_A^{abcd}}{N_F} + 485696736\zeta_3 \frac{d_F^{abcd} d_A^{abcd}}{N_F} \\
 & + 14556672\zeta_4 \frac{d_F^{abcd} d_A^{abcd}}{N_F} - 2831980320\zeta_5 \frac{d_F^{abcd} d_A^{abcd}}{N_F} - 74649600\zeta_6 \frac{d_F^{abcd} d_A^{abcd}}{N_F} \\
 & + 2969129520\zeta_7 \frac{d_F^{abcd} d_A^{abcd}}{N_F} - 21523968 \frac{d_F^{abcd} d_A^{abcd}}{N_F} + 465813504\zeta_3^2 N_f \frac{d_F^{abcd} d_F^{abcd}}{N_F} \\
 & - 291879936\zeta_3 N_f \frac{d_F^{abcd} d_F^{abcd}}{N_F} - 6718464\zeta_4 N_f \frac{d_F^{abcd} d_F^{abcd}}{N_F} \\
 & + 380712960\zeta_5 N_f \frac{d_F^{abcd} d_F^{abcd}}{N_F} - 987614208\zeta_7 N_f \frac{d_F^{abcd} d_F^{abcd}}{N_F} \\
 & + 338535936 N_f \frac{d_F^{abcd} d_F^{abcd}}{N_F} \Big] \frac{a^4}{559872} + O(a^5) \tag{A2}
 \end{aligned}$$

where N_F is the dimension of the fundamental representation. Finally the tensor operator anomalous dimension in the RI' scheme is

$$\begin{aligned}
 \gamma_{\mathcal{O}'}^{\text{RI}'}(a, \alpha) = & C_F a + [9\alpha^2 C_A + 27\alpha C_A + 257C_A - 171C_F - 52N_f T_F] \frac{C_F a^2}{18} \\
 & + [162\alpha^4 C_A^2 + 1215\alpha^3 C_A^2 + 324\alpha^3 C_A C_F + 5715\alpha^2 C_A^2 + 972\alpha^2 C_A C_F \\
 & - 1440\alpha^2 C_A N_f T_F + 16902\alpha C_A^2 - 6264\alpha C_A N_f T_F - 92448\zeta_3 C_A^2 \\
 & + 213548C_A^2 + 167616\zeta_3 C_A C_F - 228744C_A C_F + 13824\zeta_3 C_A N_f T_F \\
 & - 99536C_A N_f T_F - 41472\zeta_3 C_F^2 + 39420C_F^2 - 24192\zeta_3 C_F N_f T_F \\
 & + 45576C_F N_f T_F + 9152N_f^2 T_F^2] \frac{C_F a^3}{648} \\
 & + \left[3645\alpha^6 C_A^3 C_F + 40824\alpha^5 C_A^3 C_F + 8748\alpha^5 C_A^2 C_F^2 + 272403\alpha^4 C_A^3 C_F \right. \\
 & + 49572\alpha^4 C_A^2 C_F^2 - 38880\alpha^4 C_A^2 C_F N_f T_F + 11664\alpha^4 C_A C_F^3 + 24786\zeta_3 \alpha^3 C_A^3 C_F \\
 & + 1104192\alpha^3 C_A^3 C_F + 23328\zeta_3 \alpha^3 C_A^2 C_F^2 + 210924\alpha^3 C_A^2 C_F^2 \\
 & - 309096\alpha^3 C_A^2 C_F N_f T_F - 46656\zeta_3 \alpha^3 C_A C_F^3 + 81648\alpha^3 C_A C_F^3 \\
 & - 77760\alpha^3 C_A C_F^2 N_f T_F - 319788\zeta_3 \alpha^2 C_A^3 C_F - 38880\zeta_5 \alpha^2 C_A^3 C_F \\
 & + 4203198\alpha^2 C_A^3 C_F + 299376\zeta_3 \alpha^2 C_A^2 C_F^2 + 365472\alpha^2 C_A^2 C_F^2 \\
 & - 104976\zeta_3 \alpha^2 C_A^2 C_F N_f T_F - 2033856\alpha^2 C_A^2 C_F N_f T_F - 334368\zeta_3 \alpha^2 C_A C_F^3 \\
 & + 316872\alpha^2 C_A C_F^3 + 311040\zeta_3 \alpha^2 C_A C_F^2 N_f T_F - 645408\alpha^2 C_A C_F^2 N_f T_F \\
 & + 172800\alpha^2 C_A C_F N_f^2 T_F^2 + 62208\zeta_3 \alpha^2 C_F^3 N_f T_F - 62208\alpha^2 C_F^3 N_f T_F \\
 & - 2959578\zeta_3 \alpha C_A^3 C_F - 686880\zeta_5 \alpha C_A^3 C_F + 13835772\alpha C_A^3 C_F \\
 & \left. + 2541456\zeta_3 \alpha C_A^2 C_F^2 - 1253556\alpha C_A^2 C_F^2 + 990144\zeta_3 \alpha C_A^2 C_F N_f T_F \right]
 \end{aligned}$$

$$\begin{aligned}
& + 207360\zeta_5\alpha C_A^2 C_F N_f T_F - 9117360\alpha C_A^2 C_F N_f T_F - 412128\zeta_3\alpha C_A C_F^3 \\
& + 103032\alpha C_A C_F^3 - 196992\zeta_3\alpha C_A C_F^2 N_f T_F - 977184\alpha C_A C_F^2 N_f T_F \\
& - 248832\zeta_3\alpha C_A C_F N_f^2 T_F^2 + 1347840\alpha C_A C_F N_f^2 T_F^2 + 124416\zeta_3\alpha C_F^3 N_f T_F \\
& - 31104\alpha C_F^3 N_f T_F + 165888\zeta_3\alpha C_F^2 N_f^2 T_F^2 - 41472\alpha C_F^2 N_f^2 T_F^2 \\
& - 115925580\zeta_3 C_A^3 C_F + 10393920\zeta_5 C_A^3 C_F + 195274634 C_A^3 C_F \\
& + 206535744\zeta_3 C_A^2 C_F^2 + 2643840\zeta_5 C_A^2 C_F^2 - 271766556 C_A^2 C_F^2 \\
& + 53147664\zeta_3 C_A^2 C_F N_f T_F - 2177280\zeta_5 C_A^2 C_F N_f T_F - 144291864 C_A^2 C_F N_f T_F \\
& - 41570496\zeta_3 C_A C_F^3 - 34525440\zeta_5 C_A C_F^3 + 87039360 C_A C_F^3 \\
& - 84001536\zeta_3 C_A C_F^2 N_f T_F + 6220800\zeta_5 C_A C_F^2 N_f T_F + 115518384 C_A C_F^2 N_f T_F \\
& - 5391360\zeta_3 C_A C_F N_f^2 T_F^2 + 30575616 C_A C_F N_f^2 T_F^2 - 15552000\zeta_3 C_F^4 \\
& + 24883200\zeta_5 C_F^4 - 10195308 C_F^4 + 12317184\zeta_3 C_F^3 N_f T_F \\
& - 4976640\zeta_5 C_F^3 N_f T_F - 10896768 C_F^3 N_f T_F + 7050240\zeta_3 C_F^2 N_f^2 T_F^2 \\
& - 10107648 C_F^2 N_f^2 T_F^2 - 1744384 C_F N_f^3 T_F^3 + 1617408\zeta_3 \frac{d_F^{abcd} d_A^{abcd}}{N_F} \\
& - 4976640\zeta_5 \frac{d_F^{abcd} d_A^{abcd}}{N_F} - 248832 \frac{d_F^{abcd} d_A^{abcd}}{N_F} - 746496\zeta_3 N_f \frac{d_F^{abcd} d_F^{abcd}}{N_F} \\
& + 2985984 N_f \frac{d_F^{abcd} d_F^{abcd}}{N_F} \Big] \frac{a^4}{23328} + O(a^5) \tag{A3}
\end{aligned}$$

for an arbitrary linear covariant gauge. The one loop term is clearly scheme independent.

-
- [1] G. Buchalla *et al.*, *Eur. Phys. J. C* **57**, 309 (2008).
[2] M. Antonelli *et al.*, *Phys. Rep.* **494**, 197 (2010).
[3] T. Blake, G. Lanfranchi, and D. M. Straub, *Prog. Part. Nucl. Phys.* **92**, 50 (2017).
[4] J. De Blas, Y. Du, C. Grojean, J. Gu, V. Miralles, M. E. Peskin, J. Tian, M. Vos, and E. Vryonidou, [arXiv:2206.08326](https://arxiv.org/abs/2206.08326).
[5] G. Martinelli, C. Pittori, C. T. Sachrajda, M. Testa, and A. Vladikas, *Nucl. Phys.* **B445**, 81 (1995).
[6] E. Franco and V. Lubicz, *Nucl. Phys.* **B531**, 641 (1998).
[7] J. A. Gracey, *Nucl. Phys.* **B662**, 247 (2003).
[8] C. Sturm, Y. Aoki, N. H. Christ, T. Izubuchi, C. T. C. Sachrajda, and A. Soni, *Phys. Rev. D* **80**, 014501 (2009).
[9] M. Gorbahn and S. Jäger, *Phys. Rev. D* **82**, 114001 (2010).
[10] L. G. Almeida and C. Sturm, *Phys. Rev. D* **82**, 054017 (2010).
[11] J. A. Gracey, *Eur. Phys. J. C* **71**, 1567 (2011).
[12] V. M. Braun, T. Burch, C. Gatteringer, M. Göckeler, G. Lacagnina, S. Schaefer, and A. Schäfer, *Phys. Rev. D* **68**, 054501 (2003).
[13] T. Bhattacharya, V. Cirigliano, R. Gupta, H.-W. Lin, and B. Yoon, *Phys. Rev. Lett.* **115**, 212002 (2015).
[14] T. Bhattacharya, V. Cirigliano, S. D. Cohen, R. Gupta, H.-W. Lin, and B. Yoon, *Phys. Rev. D* **94**, 054508 (2016).
[15] M. Abramczyk, S. Aoki, T. Blum, T. Izubuchi, H. Ohki, and S. Syritsyn, *Phys. Rev. D* **96**, 014501 (2017).
[16] C. Pena and D. Preti, *Eur. Phys. J. C* **78**, 575 (2018).
[17] T. Harris, G. von Hippel, P. Junnarkar, H. B. Meyer, K. Ottnad, J. Wilhelm, H. Wittig, and L. Wrang, *Phys. Rev. D* **100**, 034513 (2019).
[18] D. Hatton, C. T. H. Davies, G. P. Lepage, and A. T. Lytle, *Phys. Rev. D* **102**, 094509 (2020).
[19] F. He, Y.-J. Bi, T. Draper, K.-F. Liu, Z. Liu, and Y.-B. Tang, [arXiv:2204.09246](https://arxiv.org/abs/2204.09246).
[20] R. Tsuji, N. Tsukamoto, Y. Aoki, K.-I. Ishikawa, Y. Kuramashi, S. Sasaki, E. Shintani, and T. Yamazaki, [arXiv:2207.11914](https://arxiv.org/abs/2207.11914).
[21] P. Gambino, M. Gorbahn, and U. Haisch, *Nucl. Phys.* **B673**, 238 (2003).
[22] P. A. Baikov and K. G. Chetyrkin, *Nucl. Phys. B, Proc. Suppl.* **160**, 76 (2006).
[23] S. G. Gorishny, S. A. Larin, L. R. Surguladze, and F. K. Tkachov, *Comput. Phys. Commun.* **55**, 381 (1989).
[24] S. A. Larin, F. V. Tkachov, and J. A. M. Vermaseren, The form version of Mincer, NIKHEF-H-91-18 (NIKHEF, Amsterdam, The Netherlands, 1991).
[25] J. A. M. Vermaseren, [arXiv:math-ph/0010025](https://arxiv.org/abs/math-ph/0010025).

- [26] M. Tentyukov and J. A. M. Vermaseren, *Comput. Phys. Commun.* **181**, 1419 (2010).
- [27] T. Ueda, B. Ruijl, and J. A. M. Vermaseren, *Proc. Sci., LL2016* (2016) 070.
- [28] T. Ueda, B. Ruijl, and J. A. M. Vermaseren, *Comput. Phys. Commun.* **253**, 107198 (2020).
- [29] P. Nogueira, *J. Comput. Phys.* **105**, 279 (1993).
- [30] T. van Ritbergen, A. N. Schellekens, and J. A. M. Vermaseren, *Int. J. Mod. Phys. A* **14**, 41 (1999).
- [31] S. A. Larin and J. A. M. Vermaseren, *Phys. Lett. B* **303**, 334 (1993).
- [32] G. 't Hooft, *Nucl. Phys.* **B61**, 455 (1973).
- [33] W. E. Caswell and F. Wilczek, *Phys. Lett.* **49B**, 291 (1974).
- [34] F. Herzog, B. Ruijl, T. Ueda, J. A. M. Vermaseren, and A. Vogt, *J. High Energy Phys.* **02** (2017) 090.
- [35] T. Luthe, A. Maier, P. Marquard, and Y. Schröder, *J. High Energy Phys.* **10** (2017) 166.
- [36] K. G. Chetyrkin, G. Falcioni, F. Herzog, and J. A. M. Vermaseren, *J. High Energy Phys.* **10** (2017) 179.
- [37] K. G. Chetyrkin and A. Rétey, *Nucl. Phys.* **B583**, 3 (2000).
- [38] D. J. Broadhurst and A. G. Grozin, *Phys. Rev. D* **52**, 4082 (1995).
- [39] J. A. Gracey, *Phys. Lett. B* **488**, 175 (2000).
- [40] J. Blümlein, P. Marquard, C. Schneider, and K. Schönwald, *Nucl. Phys.* **B971**, 115542 (2021).
- [41] J. A. Gracey, 2022 data, arXiv, <https://doi.org/10.48550/arXiv.2208.14527> (2022).